Protein−Poly(silicic) Acid Interactions at The Air/Solution Interface

Mark J. Henderson, Adam W. Perriman, Hana Robson-Marsden, and John W. White*

Research School of Chemistry, Australian National University, Canberra 0200, Australia

Received: April 13, 2005; In Final Form: September 2, 2005

The structure of the interface generated by a spread layer of β-casein on an aqueous colloidal poly(silicic) acid subphase is described. The results are compared with data for the protein alone spread at the air/water interface and the silicate solution. Films develop at the air−solution interface and a strong pH dependence of the interaction causing this is demonstrated. Reflectometry with X-rays and neutrons was used to probe the interaction as a function of subphase pH and film compression. Film thickness, τ/Å, scattering length density, ρ/Å^{-2}, water volume fraction, φ_w, and surface coverage, Γ/mg m^{-2}, were used to quantify the interfacial structure. Where possible, the X-ray and neutron data sets were co-refined enabling φ_w to be evaluated without assumption regarding the protein density. At pH 5−7, strong protein−silicate interaction occurred, the interface comprising three regions: a discrete protein upper layer on top of a 15 ± 2 Å layer of silicated material followed by a diffuse layer that extended into the subphase.

1. Introduction

We have explored the structure of the interface that develops visibly when β-casein was spread on a poly(silicic) acid subphase. Clark et al. described surface balance studies of the effect of aqueous poly(silicic) acid, generated from sodium metasilicate solution, on monomolecular layers of insulin, albumin, and polyamides (nylon) on the surface of the solution.[1] Poly(silicic) acid was adsorbed on the underside of the organic layer. It is this type of simple monolayer system that we examine at nanometer resolution as a model for self-assembled biomolecular materials.[2]

Recently, the specific effect of amino acids,[3] polyamines,[4,5] peptides,[3] proteins,[6] mixed lipid−protein monolayers,[7−9] and biosilica extracts[10−16] on the polymerization of silicic acid was investigated. The amino acids serine, lysine, proline, and aspartic acid were found to facilitate the polymerization. For example, bovine serum albumin (BSA) was shown to control silica particle size, thereby mimicking a natural biosilicification process.[6] Protein extracts, isolated from diatom cell walls, have been shown to generate networks of silica spheres within seconds when added to a solution of silicic acid.[14] These silica-precipitating peptides, known as silaffins, were shown to contain a high loading of positively charged polyamine side chains that accelerate silica condensation under neutral or mildly acidic conditions.[13]

Silica is the condensation polymer of monosilicic acid, $Si(OH)_4$. The formation of monosilicic acid,[17] its polymerization,[18,19] and behavior[20] are relevant to the present work. Monosilicic acid can be kept for a measurable time at pH 2 or 3; the point of minimum stability is at pH 5.5, significantly above the isoelectric point (IEP) of silica, pH 2−3.[21] When polymerized, there is no distinction between the highly condensed poly(silicic) acids and colloidal silica.[22] Measured densities of poly(silicic) acids derived from acidification of aqueous sodium metalsilicate solutions are dependent on acid concentration and are reported to fall in the range 1.6−2.0 g cm^{-3},[23] lower than that of fully condensed SiO_2, 2.2 g cm^{-3}.

* To whom correspondence should be addressed. E-mail: jww@rsc.anu.edu.au. Phone: +61 (02) 6125-3578. Fax: +61 (02) 6125-4903.

β-Casein is a single-chain protein of 209 residues[24] and molecular weight 24 It is flexible and water soluble with no disulfide linkages and has an isoelectric point at pH 4.5[25] The N-terminal part of the β-casein molecule (residues 1 to 40) contains the phosphoserine residues and possesses most of the protein's potential charge. The net charge at neutral pH is −16.[26] The C-terminal part of the molecule (residues 136 to 209) contains many apolar residues imparting a hydrophobic character. Flexible linear molecules, such as β-casein, have been considered as polymer-like,[27] represented by a classical train-loop model when adsorbed at the solid/water[28] or air/water interface.[29,30] The location of the loops and segments at the oil/water interface was the focus of a recent Monte Carlo simulation.[31] Here, we examine the structure of protein−silica films with reflectometry using X-rays and neutrons. The use of multiple contrasts in this way enables the scattering from the protein and the subphase to be decoupled to allow the surface excess of protein and volume fraction of water at the interface to be evaluated without assumptions regarding the volume of the protein.

2. Experimental Procedures

2.1. Materials. Two sources of β-casein were used: (a) a product of nearly 100% purity as demonstrated by HPLC and (b) a sample of 90% purity (Sigma).

The high-purity β-casein was prepared from whole milk from an individual cow. This was skimmed by centrifuging at 2000 g for 15 min at 25 °C. The casein was prepared at room temperature (20−25 °C) by a double acid precipitation at pH 4.6.[32] Skim milk (2 L) was adjusted to pH 4.6 with 1 mol dm^{-3} HCl and stirred for 30 min. After centrifugation at 3000 rpm for 15 min at 25 °C, the whey was discarded and the pellet re-suspended in 2 L of 5 mmol dm^{-3} sodium acetate buffer, pH 4.6, containing 0.02% sodium azide for 15−30 s. The suspension was stirred for 30 min, centrifuged and the pellet again dispersed in acetate buffer at pH 4.6. The pH of the mixture was continually adjusted to pH 7.0 with 1 mol dm^{-3} NaOH and the casein allowed to completely redissolve overnight. Precipitation of the casein at pH 4.6 was repeated and,

10.1021/jp051908k CCC: $30.25
Published on Web 10/12/2005

after centrifugation, the pellet was dispersed in 1 L of deionized water containing 0.02% sodium azide and redissolved at pH 7.0. The casein was freeze-dried and stored at −20 °C.

Ion exchange chromatography was performed on a cation-exchange resin S-Sepharose Fast Flow according to Leaver and Law.[33] A 26 × 400 mm^2 column was packed at 3.5 mL min^{-1} to a bed height of 250 mm and equilibrated at 4 °C in phase A, 20 mmol dm^{-3} sodium acetate pH 5.0 containing 6 mol dm^{-3} urea. Whole casein (2.0 g) was dissolved in phase A (100 mL) to which β-mercaptoethanol (200 μL) was added and the pH adjusted to 7.0 with 1 mol dm^{-3} NaOH. After standing for 1 h at room temperature, the pH was adjusted to 5.0 with 1 mol dm^{-3} HCl. The sample was loaded at 3.5 mL min^{-1} and washed with 140 mL of phase A followed by a step gradient of 10−40% phase B (1400 mL), 40−100% phase B (70 mL), and 280 mL of 100% B. (Phase B comprised phase A with 1 mol dm^{-3} NaCl.) The gradient was formed with a gradient programmer (Pharmacia GP-250) and fractions (20 mL) were collected with a Superac fraction collector. Preparative reverse-phase HPLC was done with a Shimadzu LC8A preparative HPLC system, using a protein C4 (Vydac 214TP1022; 22 × 250 mm^2, 10 mm particle size) column. Mobile phases were the following: phase A, 0.1% TFA; phase B, 60% acetonitrile in 0.085% TFA. The flow rate during separation was 22 mL min^{-1}. Elution of protein and peptides was monitored at 214 and 280 nm.

2.2. Film Formation. For each experiment involving β-casein (whether pure or 90%), a 30 μL aliquot of a 1 mg mL^{-1} solution of the protein (dissolved in 60% (v/v) 2-propanol + 0.5 mol dm^{-3} sodium acetate solution) was spread by syringe onto either Milli-Q quality water or a poly(silicic) acid subphase.

For the experiments a poly(silicic) acid subphase at pH 2−3 (where the subphase is stable with respect to polymerization) and at pH 5−7 (where further polymerization of poly(silicic) acid is facilitated) was studied.[21] The rate of polymerization of silicic acid depends on pH and, except in the range pH 5.5−6, is slow.[34] To make the subphases, a sol was prepolymerized at ca. pH 6.0 before being brought to the required pH to avoid complications arising from the polymerization reaction. An aqueous solution was prepared by adding 2 mol dm^{-3} HCl solution dropwise to a stirred aqueous solution of $Na_2SiO_3 \cdot 9H_2O$ (0.025 mol dm^{-3}) to pH 5−7. The solution was stirred for 1 h at 25 °C. Poly(silicic) acid at pH 2−3 was prepared by stabilizing a prepared solution of the poly(silicic) acid at pH 5−7 with 2 mol dm^{-3} HCl. The slightly turbid sols were used immediately after preparation. To avoid complications from other anions, the subphase was not buffered.

2.3. Surface Balance. In all experiments involving protein, pressure−area (π−A) isotherms at 25 °C were obtained from a spread layer. Surface measurements were made by using a fully automated Langmuir trough (Nima 601). The subsolution temperature was controlled by water circulation from a thermostat-controlled bath. Spreading was achieved by forming droplets at the tip of a syringe (Hamilton) and touching the subphase with the droplets. A PTFE barrier could be moved to modify the area of the trough and, hence, the surface concentration of the spread β-casein at a compression rate of 40 cm^2 min^{-1}. Though X-ray reflectivity measurements were performed simultaneously with surface film measurements, measurements with neutrons involved two different instruments and are therefore sequential experiments.

2.4. Reflectometry and Data Analysis. The X-ray measurements were performed on an angle dispersive reflectometer described elsewhere.[35] The Cu Kα radiation was selected by using a flat graphite (002) monochromator. Measurements were made at angles of incidence in the range 0.0−3.4° (0.00−0.48 Å^{-1}). The alignment of the reflectometer with respect to the liquid surface was confirmed by measuring the reflectivity of a sample of Millipore quality water and comparing the observed model parameters, with established values. Measurements were commenced as soon as possible after spreading the protein and once alignment of the liquid surface with the incident beam was achieved, typically 20 min. However, as the time scales of experiments were quite short, <1.5 h on some subphases, e.g., poly(silicic) acid subphase, pH 5−7, the interfacial structure may have not reached equilibrium during the experiments.

The neutron reflectivity profiles were measured at the CRISP reflectometer of the ISIS spallation neutron source at the Rutherford Appleton Laboratory, Oxfordshire, UK. The data were collected with the beam incident on the sample at angles of 0.8° and 1.5°. The alignment of the reflectometer was confirmed by measuring the reflectivity of a sample of D_2O and comparing the observed model parameters, with established values. In a typical experiment, on the CRISP reflectometer, reflectivity can be measured over a Q_z range of 0.03−0.25 Å^{-1}. However, the minimum measurable reflectivity is restricted by the incoherent background scattering from the sample. Consequently, only the data up to 0.125 Å^{-1} were modeled. An aqueous poly(silicic) acid subphase solution was prepared to be null reflecting so that only the interface was highlighted. The null reflecting subphase was a mixture of H_2O and D_2O and silica so that the final scattering length density matched that of air. The air−liquid interface reflectometry was performed in a temperature-controlled sealed trough at 25 °C.

The data from X-ray and neutron reflectivity were then modeled with use of CXMULF, a program based on the optical transfer matrix method of classical optics as described by Penfold[36] and illustrated by Brown et al.[37] The method uses the approach that the interfacial structure can be described as one or more layers. A simulated annealing least-squares approach was then used to minimize the difference between the model and the data. The model parameters used are the film thickness (τ/Å), scattering length density (ρ/Å^{-2}), and a Gaussian interfacial roughness (σ/Å). For these experiments the subphase scattering length density and the interfacial roughness were constrained between the X-ray and neutron data sets allowing the film scattering length density and thickness to be fitted.

2.5. Methodology. The surface coverage, Γ (g m^{-2}), was evaluated for the protein at an interface when neutron reflectivity is performed on a subphase contrast-matched with air. In this case the protein surface coverage can be obtained from eq 1[38]

$$\Gamma = \frac{10^{20} M_w \rho_N \tau}{N_A \sum b_{prot}} \quad (1)$$

where M_w is the molecular weight of the protein (g mol^{-1}), ρ_N is the measured scattering length density of the layer, N_A is Avogadro's number, τ is the layer thickness, and $\sum b_{prot}$ is the sum of the scattering length of the elements which make up the protein (Å), allowing for isotopic exchange. Equation 1 is valid for a protein unaltered from its solution conformation at the interface, for example when the protein has not denatured. Once the protein volume has been obtained it is then possible to derive the water content within the protein. If the protein has altered from its solution conformation, the situation requires the use of a different contrast, e.g., X-ray reflectivity, and this has been done to find the volume fraction of water in an analogous way to myoglobin.[38] Equation 1 has been developed assuming a single layer with one average scattering length

density. The assumption of a homogeneous layer is based on the resolution of the neutron experiment. The Q_z range defines the resolution available in the scattering experiment as follows, resolution $= 2\pi/Q_{z\,\max}$, i.e., the resolution is 20 Å or larger depending upon the incoherent background scattering. At this low resolution of the neutron experiment, the condition of uniform layer distribution of β-casein, a highly disordered protein, is justified. However, as a result of the larger Q_z range possible with X-ray reflectivity, a refinement to the model can be made if the neutron measurements are made in combination with X-ray reflectivity measurements, as used in the present study. It is an accepted practice to begin modeling by testing the fit to the data of a single uniform layer. Following this practice and looking ahead to Table 4, we obtained a single 13 Å layer fit for the most straightforward system studied, an as-spread film of β-casein spread at the air−water interface. That the single uniform layer model fits these data supports the assumption of a homogeneous layer within the resolution of the X-ray experiment.

A a null-reflecting subphase also allows the average volume occupied by a protein at the interface, V_{prot} (molecules Å^{-3}) to be accessed by using eq 2.

$$V_{\text{prot}} = \frac{\sum b_{\text{prot}}}{\rho_{\text{N}}} \tag{2}$$

An X-ray scattering length density of the protein denoted ρ'_x is then obtained from a consideration of V_{prot} derived from the neutron experiment,

$$\rho'_x = \frac{\sum e_{\text{prot}} r_0}{V_{\text{prot}}} \tag{3}$$

where $\sum e_{\text{prot}}$ is the number of electrons in a single protein molecule and r_0 is the classical electron radius. The derived ρ'_x is then compared with the measured X-ray scattering length density, ρ_x, allowing the volume fraction of water, φ_{w}, to be determined,

$$\phi_{\text{w}} = \frac{\rho_x - \rho'_x}{\rho_{\text{water}}} \tag{4}$$

Where an interaction between the protein and poly(silicic) acid occurs, the X-ray scattering length density of the protein−silica hybrid must be included in the volume fraction,

$$\phi_{\text{w}} = \frac{\rho_x - \rho'_{\text{protein-silica}}}{\rho_{\text{water}}} \tag{5}$$

The interaction decreases φ_{w}, and increases the surface excess, Γ, beyond what would be expected for an interface consisting of only protein and water. For uniformity throughout this paper, the water volume fraction, φ_{w}, was calculated assuming that only protein and water were present at the interface as the stoichiometry of the protein−silica complex (and hence a derived ρ'_x) was not known. That is, eq 4 was used to extract φ_{w}. Volume fractions were then compared with values derived from a conventional method,[39]

$$\rho_{\text{layer}_{(z)}} = \phi_{\text{protein}_{(z)}} \rho_{\text{protein}} + (1 - \phi_{\text{protein}_{(z)}}) \rho_{\text{water}} \tag{6}$$

This was achieved by using a layer scattering length density, $\rho_{\text{layer}_{(z)}}$, obtained from X-ray reflectivity measurements. A protein scattering length density, ρ_{protein}, was computed from the sum of the scattering lengths of the constituent atoms,

$$\rho_{\text{protein}} = \sum_i^N b_i \times \frac{D \times N_{\text{A}}}{M_{\text{w}}} \tag{7}$$

where b_i is the scattering length of atom i, N is the total number of atoms in the protein molecule, N_{A} is Avogadro's number, M_{w} is the molecular weight, and D is the protein density. The protein density was derived from an approximation of the total volume of the protein from amino acid residues, Table 1.[40] The extent of the effect of the formation of the protein silica complex is discussed in Section 3.5 (below).

TABLE 1: Properties of Materials

	β-casein
mol wt	23626 (monomer)
density D^a/g cm^{-3}	1.333
isoelectric point^b (IEP)	4.5
scattering length^c b/Å	521.2×10^{-4}
X-ray SLD ρ/Å^{-2}	12.12×10^{-6}
neutron SLD ρ/Å^{-2}	
no exchange	1.77×10^{-6}
ACMW^d exchange	1.88×10^{-6}
D_2O exchange	2.85×10^{-6}

[a] Density from protein specific volume calculated from constituent amino acid residues, from ref 54. [b] Isoelectric points, from ref 25. [c] Scattering length calculated from constituent atoms and known neutron scattering lengths.[55] [d] ACMW is air contrast-matched water.

3. Results

3.1. Control Experiments on β-Casein Spread at the Air/Water Interface, pH 2−3 and 5−7. Prior to exploring the interaction of the protein at the air/poly(silicic) acid interface, the reflectivity profiles from β-casein spread at the air/water interface were recorded. The X-ray RQ_z^4 vs Q_z plots of β-casein (near 100% purity) spread at the air/water interface, pH 2−3 and 5−7, are shown in Figure 1a,b. The modeled reflectivity for the expanded and compressed films shown is represented by a line through each profile and by the parameters shown in Table 2. For the protein at each pH, the structures of the uncompressed (trough area ca. 500 cm^2) and a partly compressed film (trough area ca. 150 cm^2) were examined. For the uncompressed films the interfacial structure at either pH consists of only a single layer of thickness 11−14 Å with a scattering length density between that of water (9.43×10^{-6} Å^{-2}) and the calculated value for β-casein (12.12×10^{-6} Å^{-2}) Table 1. The film data were best fitted with an additional layer that extended into the subphase. Where an interface comprising multiple layer was indicated, the total thickness of the film was between 30 and 33 Å.

3.2. Control Experiment on the Reflectivity of Air/Poly-(silicic) Acid Interface. The measured X-ray reflectivity profiles of the air/poly(silicic) acid interface at pH 2−3 and 5−7 are displayed in Figure 2, parts a and b, respectively, as RQ_z^4 vs Q_z plots (closed circle). A comparison of the profiles with that of the air/water interface (open circle) is also shown. A neutron reflectivity profile of a poly(silicic) acid subphase contrast-matched to air by using a mixture of D_2O and H_2O showed no reflectivity (profile not shown). The measured signals were characteristic of background radiation levels over the Q_z range studied. The modeled reflectivity of the interfaces at each pH is represented by the parameters presented in Table 3. For each pH, we obtained for the poly(silicic) acid subphase a scattering length density (SLD) and roughness (σ) similar to the values for the air−water interface when the interface was modeled with

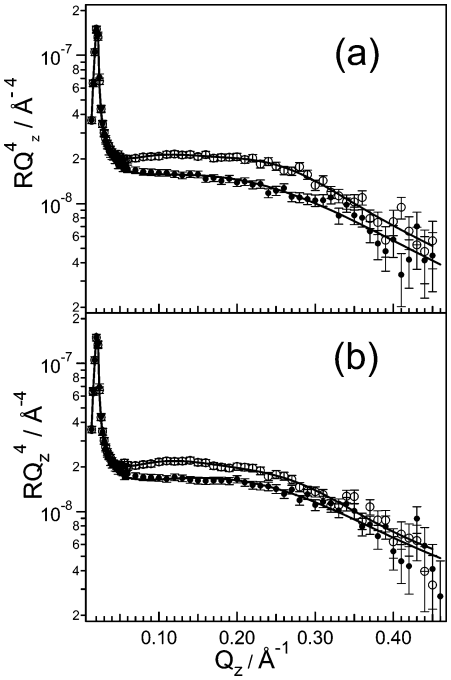

Figure 1. Measured X-ray RQ_z^4 vs Q_z profiles of β-casein spread at the air/water interface at (a) pH 2−3 and (b) 5−7 uncompressed (solid circle) and compressed (open circle). The line through each profile represents the modeled reflectivity. The parameters obtained are shown in Table 2.

no layers. Although the SLD and film roughness, σ, values are in close agreement with those obtained from the air/water interface, a marginal improvement of the fit was obtained by applying a one-layer model with a layer thickness of 4 Å. As this value is close to the resolution of the instrument and no surface activity was detected by a surface balance study, a zero-layer model was adopted. The subphase SLD for water was used (and constrained) in all subsequent models for this subphase when fitting X-ray reflectivity data. The $\pi-A$ isotherms from each air/poly(silicic) acid subphase, displayed as insets to Figure 2, were featureless over the trough areas studied.

3.3. β-Casein Spread at the Air/Poly(silicic) Interface, pH 2−3. The comparison between the measured X-ray RQ_z^4 vs Q_z profiles of β-casein spread at the air/poly(silicic) acid interface at pH 2−3 for the surface areas 500 and 150 cm^2 is presented in Figure 3, parts a and b, respectively. In each case the profile obtained from the air/water and the air/poly(silicic) acid interfaces at the associated pH is shown for comparison. The line through each profile represents the modeled reflectivity. Table 4 of the set presents φ_p derived by using X-ray data only and eq 6. Looking ahead to the corefinement of the X-ray and neutron data, Table 5 presents φ_w and surfaces coverage, Γ, derived by using the null reflecting subphase.

3.4. Corefinement of X-ray and Neutron Data. *β-Casein (trough area 500 cm^2).* For β-casein, the X-ray and neutron reflectivity measurements (Table 5) were able to be corefined. This interface comprises only a single 13 Å protein-rich layer, significantly less than that reported for adsorbed β-casein at the air/water interface.[39,41] We have inferred that the 13 Å layer corresponds to the hydrophobic densely packed part of the protein, the lower hydrophilic region being too diffuse for a layer to be revealed by neutron reflectivity.

β-Casein (trough area ca. 150 cm^2). Figure 4 shows (a) X-ray and (b) neutron RQ_z^4 vs Q_z profiles obtained from β-casein spread at the air/poly(silicic) acid interface at pH 2−3, trough area ca. 150 cm^2, showing the comparison of one-layer and two-layer fits to the data. A distinct difference is to be noted around $Q_z \approx 0.04-0.1$ Å^{-1}. As noted, three model parameters, film thickness (τ/Å), scattering length density (ρ/Å^{-2}), and a Gaussian interfacial roughness (σ/Å), are allowed to fit during the refinement. For a complex interface, e.g., one containing multiple layers, the model can become over parametrized leading to nonunique solutions to the fit. In all cases presented in this work the data were first fitted by using a one-layer model. Where large standard deviations were encountered with use of a one-layer fit, an additional layer was added to the model and so on. The best fit to the data in this case is the two-layer model, $\chi = 0.97$ (cf. one-layer model $\chi = 2.2$). As Table 5 suggests, the refined protein surface coverage of 3.3 mg m^{-2} overestimates the amount applied to this subphase, 2.0 mg m^{-2}. However, as the surface excess was derived by using eq 1 assuming an interface comprising only protein and water, the result indicates the presence of siliceous material at the interface.

3.5. β-Casein Spread at the Air/Poly(silicic) Interface, pH 5−7. The measured X-ray RQ_z^4 vs Q_z profiles of β-casein spread air/poly(silicic) acid interface at pH 5−7 are presented in Figure 5 for (a) the uncompressed film, trough area ca. 500 cm^2, and (b) a partly compressed film, trough area ca. 200 cm^2. A comparison of the profile obtained from air/water and air/poly-(silicic) acid interface at the associated pH is shown for comparison. The line through each profile represents the modeled reflectivity. The parameters obtained from the fitting and the extracted volume fraction of protein, φ_p, in each layer are shown in Table 4 (X-ray analysis). Table 5 (X-ray and neutron analysis) presents the parameters from the fit and the volume fraction of water, φ_w, for β-casein spread at this interface. Figure 6 shows a comparison of (a) the X-ray and (b) the neutron data for β-casein on poly(silicic) acid subphase at pH 5−7 for the film in the uncompressed state and Figure 7 the X-ray data when the film was compressed illustrating the rather better fit to the fringe at low Q_z found when a three-layer model was used. The disagreement in the number of layers for X-rays and neutrons is caused by the restricted Q_z range provided by neutron data, a result of the high incoherent background that is reached at relatively low Q_z values. Therefore only the larger scale structures of this interface, including the upper and lower boundaries of the interface, were defined. Figure 6b shows the comparison of the one- and two-layer models used to fit the neutron data, from which the two-layer model was chosen. To enable the two-layer model to be corefined with the three-layer model obtained from X-ray data, the two-layer model obtained from neutron measurements was further subdivided into three layers based on the thicknesses from the X-ray model. The partitioning of the interface required the first two layers to have the same neutron scattering length density. Since the partition is an artificial one, the scattering length densities applied to the partitioned layers were constrained to the value obtained from a fit to the neutron data obtained prior to the corefinement.

The interface is more clearly revealed by Figure 8, which shows scattering length density (ρ) vs depth (τ) profiles from an uncompressed film of β-casein spread at the air/poly(silicic) acid (closed circle) and at the air/water interface (open triangle) at pH 5−7. The profile obtained from the air/poly(silicic) interface, pH 5−7, without spread protein (open circle) is shown. The line through each profile represents the modeled data. On scattering length density grounds, and after a consideration of the chemistry possible at this interface, we interpret this middle layer to contain predominantly silica, gelled locally beneath the protein.

TABLE 2: X-ray Reflectivity Fits for β-Casein Spread at the Air/Water Interface

pH	area/ cm^2	layer	τ/ Å	$10^{-6}\rho_x$/ Å^{-2}	φ_p	$\Gamma_{per\ layer}$/ mg m^{-2}	$\Gamma_{applied}$/ mg m^{-2}	Γ_{total}/ mg m^{-2}
2−3	498	1	12.90(1.5)	10.27(0.15)	0.30(0.05)	0.52(0.15)	0.60	0.52(0.15)
2−3	149	1	13.05(0.6)	11.68(0.11)	0.79(0.04)	1.40(0.13)	2.01	1.80(0.21)
		2	20.43(1.6)	9.85(0.05)	0.15(0.02)	0.41(0.08)		
5−7	498	1	13.40(0.9)	10.45(0.1)	0.36(0.04)	0.65(0.11)	0.61	0.65(0.11)
5−7	149	1	13.76(0.7)	11.50(0.1)	0.73(0.04)	1.35(0.13)	2.01	1.75(0.22)
		2	16.84(1.4)	9.92(0.07)	0.17(0.02)	0.39(0.09)		

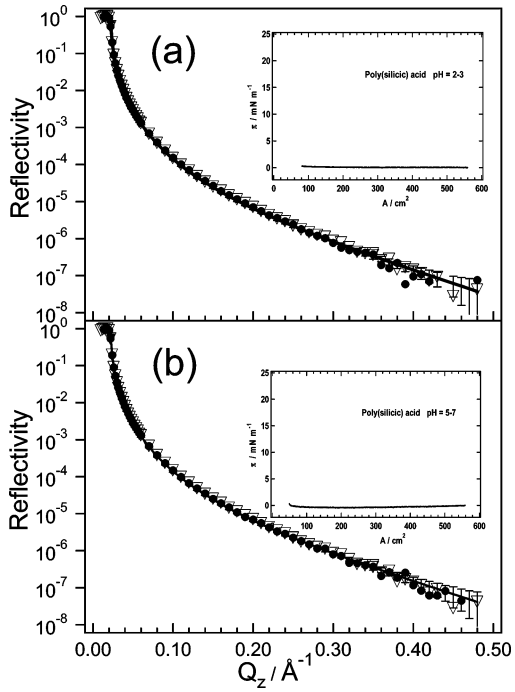

Figure 2. Measured X-ray RQ_z^4 vs Q_z profiles of (a) the air/poly-(silicic) acid interface, pH 2−3 (closed circle), and (b) the air/poly-(silicic) acid interface (pH 5−7) (closed circle). In each case a comparison of the profile obtained from the air/water interface is shown (open circle). The line through each profile represents the modeled reflectivity. The parameters obtained are shown in Table 3. Insets show the $\pi-A$ isotherm for each subphase.

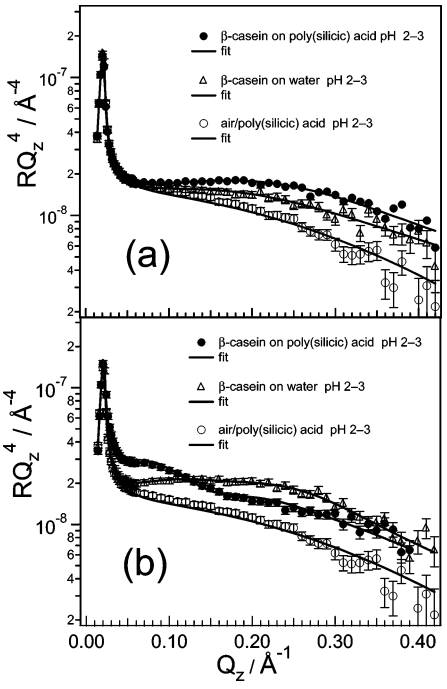

Figure 3. Comparison between the measured X-ray RQ_z^4 vs Q_z profiles of β-casein spread at the air/water and air/poly(silicic) acid interfaces at pH 2−3: (a) trough area = ca. 500 cm^2 and (b) trough area = ca. 150 cm^2. In each case a comparison of the profile obtained from the air/poly(silicic) acid interface, pH 2−3, without spread protein is shown (open circle). The line through each profile represents the modeled reflectivity. The parameters obtained are shown in Table 4.

TABLE 3: Comparison between the X-ray Reflectivity Fits for the Air/Water Interface and Air/Poly(silicic) Acid Subphases

	air-film roughness/Å	$10^{-6}\rho_x$/ Å^{-2}	quality of fit χ^2
air/water	2.9(0.3)	9.43	1.2
air/poly(silicic) acid pH 2−3	2.92(0.3)	9.59(0.04)	1.9
air/poly(silicic) acid pH 5−7	2.86(0.3)	9.52(0.03)	1.3

3.6. Features at Compression. β-casein, when spread on poly(silicic) acid subphase pH 5−7 and then compressed to a trough area of 201 cm^2, displayed a surface pressure of 17.8 mN/m. After holding in this state for 1.5 h the surface pressure had fallen to 13.1 mN/m. The rate of change of the surface pressure, ca. 0.05 mN/m/min, does suggests that some structural change at the interface occurred during the experiment. After holding in this state for 1.5 h the surface pressure had fallen to 13.1mN/m. The rate of change of the surface pressure, ca. 0.05 mN/m/min, does suggest that some structural change at the interface occurred during the experiment. At high compression the film rigidity prevented full film compression and only partly compressed films were achieved. The two uppermost layers for β-casein appear to have inverted on compressing the film. The model of a dense upper layer on top of a protein-rich layer could not be applied to any other reflectivity profiles. Figure 7 shows X-ray RQ_z^4 vs Q_z profiles showing the comparison of one-layer ($\chi^2 = 3.4$), two-layer ($\chi^2 = 1.5$), and three-layer ($\chi^2 = 1.2$) models.

3.7. The Effect of Protein Purity. A quantitative description of the interaction between a protein and the air/poly(silicic) acid interface requires a knowledge of the behavior of the protein without complications arising from the use of β-protein of ≤95% purity. For the case where we consider a significant interaction to be present, i.e., at pH 5−7, the derived thickness and densities were studied for films made with the widest purity range used in this study (≤100% purity β-casein and 90% grade β-casein). The insensitivity of the profile to any difference in the two samples is illustrated by viewing the RQ_z^4 vs Q_z plots and scattering length density profiles for films made as described above from each casein source. Figure 9a shows these data and Figure 9b the scattering length density profiles as a function of the depth. The results for the two grades of β-casein ≤100% and 90% purity are superimposed on an absolute scale. The discrepancies between the RQ_z^4 vs Q_z plots we regard as being at the margins of experimental error. In short, for the conditions at which a significant interaction exists between poly(silicic) acid and a protein, here at pH 5−7, there is no evidence to suggest any detectable differences between 100% purity β-casein and 90% grade β-casein.

TABLE 4: X-ray Reflectivity Fits for β-Casein Spread at the Air/Poly(silicic) Acid Interface

pH	area/ cm^2	layer	τ/ Å	$10^{-6}\rho_x$/Å^{-2}	φ_p	$\Gamma_{per\ layer}$/ mg m^{-2}	$\Gamma_{applied}$/ mg m^{-2}	Γ_{total}/ mg m^{-2}
2−3	498	1	13.2(0.6)	10.71(0.04)	0.45(0.02)	0.80(0.07)	0.60	0.80(0.07)
2−3	149	1	40.3(1.1)	11.87(0.05)	0.86(0.02)	4.67(0.22)	2.01	8.25(0.58)
		2	75(3)	10.43(0.06)	0.35(0.02)	3.59(0.36)		
5−7	495	1	8.4(1.0)	11.12(0.08)	0.60(0.03)	0.68(0.11)	0.61	5.13(0.73)
		2	15.6(1.5)	12.40(0.2)	1.04(0.07)	2.20(0.36)		
		3	34.4(2.0)	10.81(0.08)	0.49(0.03)	2.26(0.26)		
5−7	201	1	25.2(0.5)	12.73(0.06)	1.16(0.02)	3.95(0.13)	1.49	5.37(0.30)
		2	17(0.9)	11.08(0.1)	0.58(0.04)	1.33(0.15)		
		3	49(3)	10.06(0.1)	0.22(0.04)	0.08(0.02)		

TABLE 5: X-ray and Neutron Reflectivity Fits for β-Casein Spread at the Air/Poly(silicic) Acid Interface

pH	area/ cm^2	layer	τ/ Å	$10^{-6}\rho_n$/ Å^{-2}	V_{prot}/ Å^3	φ_w	$\Gamma_{per\ layer}$/ mg m^{-2}	$\Gamma_{applied}$/ mg m^{-2}	$\Gamma_{otal\ (ACMW)}$/ mgm^{-2}
2−3	498	1	13.2(0.6)	1.96(0.4)	$2.81 \times 10^5(5.73 \times 10^4)$	1.00(0.03)	0.18(0.04)	0.60	0.18(0.04)
2−3	149	1	40.3(1.0)	8.09(0.15)	$6.81 \times 10^4(1.26 \times 10^3)$	0.70(0.01)	2.33(0.07)	2.01	3.35(0.19)
		2	75.4(3.0)	1.90(0.2)	$2.90 \times 10^5(3.05 \times 10^4)$	0.98(0.02)	1.02(0.12)		
5−7	495	1	24.0(2.5)	7.50(0.4)	$7.34 \times 10^4(3.92 \times 10^3)$	0.76(0.03)	1.29(0.15)	0.61	2.24(0.26)
		2	35.0(2.0)	3.80(0.4)	$1.45 \times 10^5(1.53 \times 10^4)$	0.88(0.03)	0.95(0.11)		
5−7	201	1	42.4(1.0)	7.47(0.2)	$7.37 \times 10^4(1.97 \times 10^3)$	0.76(0.02)	2.26(0.08)	1.49	2.65(0.15)
		2	43.0(2.5)	1.25(0.2)	$4.40 \times 10^5(7.05 \times 10^4)$	0.99(0.02)	0.38(0.07)		

TABLE 6: Comparison of β-Casein Volume Fractions Calculated with Various Methods

pH	area/ cm^2	layer	β-casein $\varphi_p{}^a$	β-casein $\varphi_p{}^b$	β-casein $\varphi_p{}^c$
2−3	498	1	0.11	0.0	0.45
2−3	149	1	0.43	0.30	0.86
		2	0.10	0.02	0.35
5−7	495	1	0.40	0.24	0.60
		2	0.2	0.12	1.04
					0.49
5−7	201	1	0.4	0.24	1.16
		2	0.07	0.01	0.58
		3			0.22

[a] Protein volume fraction obtained from neutron measurements and assumed protein density. [b] Protein volume fraction obtained from X-ray and neutron data. [c] Protein volume fraction obtained from X-ray measurement and assumed protein density.

4. Discussion

The strong pH dependence of the interaction between poly(silicic) acid and surface spread β-casein is evident from Figure 4 (pH 2−3) and Figure 5 where the same curves are shown at pH 5−7. Furthermore, the figures show that the effect is highlighted by a factor of about 3 when the protein−silicate film is compressed. The higher compression data, shown in part b of these figures, always exhibit a prominent fringe. The fitted profiles to the protein−silicate distribution function perpendicular to the air−water interface also show evidence of a layered structure at the interface with a high silicate content. This is clearly illustrated in the maximum of the real space scattering intensity density profiles (Figure 8). The scattering length density in the region of 20 Å from the surface exceeds any expected value for protein alone. This effect has also been observed in analogous experiments on β-lactoglobulin (not shown).

Figure 10 shows a plot of net charge for β-casein and silanol oligomers as a function of pH. At pH 5−7 the proteins and poly(silicic) acid oligomers are negatively charged. Though the driving force is not clear, electrostatic interactions between locally charged domains such as those including positively charged amino acids[42] and negatively charged silicate species could facilitate condensation. We suppose that this charge difference could well be a reason for the strong interaction seen between pH 5 and 7. The formation of layered structures is reminiscent of the structures formed between charged surfactants and polyelectrolytes at the air/water interface. For example, in the early stages of the template induced formation of silicate-based films at the air−water interface, using cetyltrimethylammonium halide and hydrolyzing tetraethyl orthosilicate, a pronounced "hump" of scattering intensity appears in the reflectivity profile in the early stages of the generation of these films.[37,43] The generality of this phenomenon whereby charged surfactants interact with polyelectrolytes to form extensive layer structures beneath the air−water interface has been reported.[44−47] We suppose that something like this is happening in the case of the protein−poly(silicic) acid interaction to produce the films that we have observed.

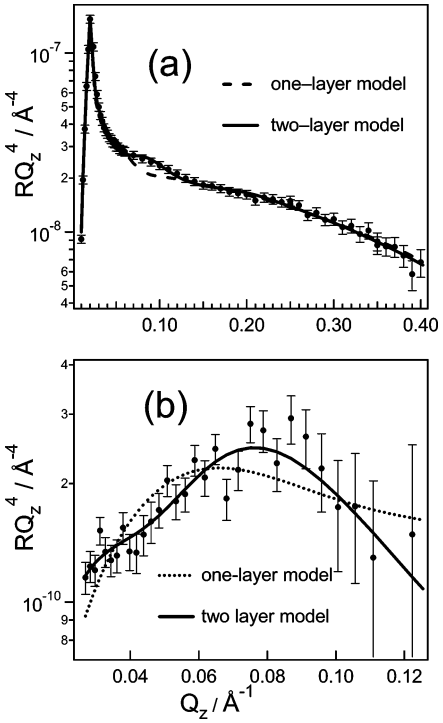

Figure 4. (a) X-ray and (b) neutron RQ_z^4 vs Q_z profiles obtained from β-casein spread at the air/poly(silicic) acid interface at pH 2−3, trough area = ca. 150 cm^2, showing the comparison of one-layer and two-layer fits to the data. The parameters obtained are shown in Table 5.

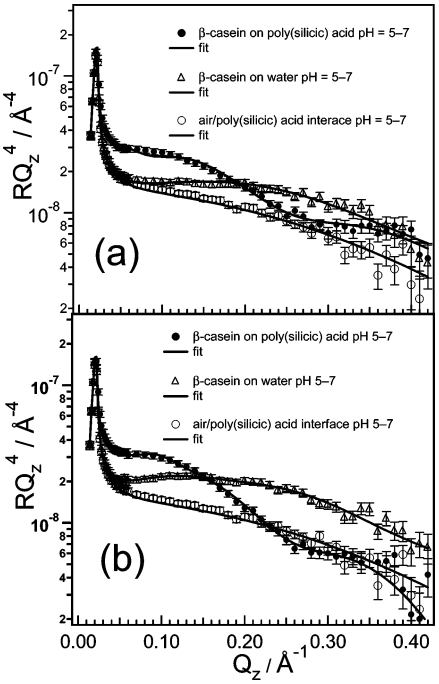

Figure 5. Comparison between the measured X-ray RQ_z^4 vs Q_z profiles of β-casein spread at the air/water and air/poly(silicic) acid interfaces at pH 5−7 (a) trough area = ca. 500 cm^2 and (b) trough area = ca. 150 cm^2. In each case a comparison of the profile obtained from the air/poly(silicic) acid interface, pH 5−7, without spread protein is shown (open circle). The line through each profile represents the modeled reflectivity. The parameters obtained are shown in Table 5.

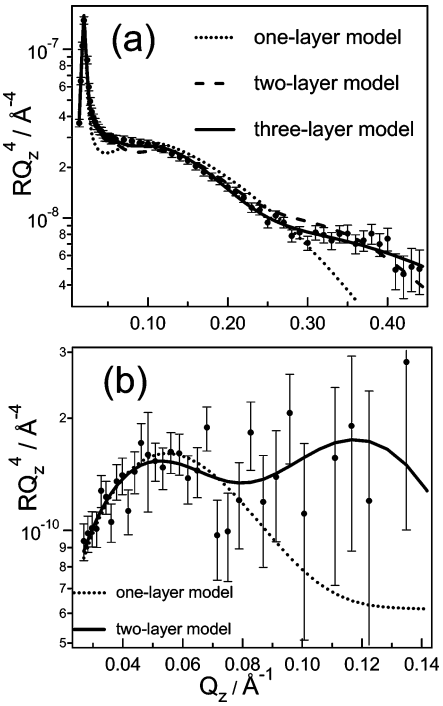

Figure 6. RQ_z^4 vs Q_z profiles obtained from β-casein spread at the air/poly(silicic) acid interface at pH 5−7, trough area ca. 500 cm^2: (a) X-ray data and (b) neutron data showing the comparison of the one-, two-, and three-layer models.

The values of water volume fraction, φ_w, from eq 4 assume that an interface is comprised of only protein and water. For conditions where siliceous material was present at the interface, the result was a decrease in φ_w, and a concomitant increase in the surface excess, Γ, beyond what would be expected for an interface consisting of protein and water. This deviation simply signaled an interaction between the protein and the poly(silicic) acid. In the case of an interaction the values obtained for φ_w therefore are affected by the presence of siliceous material. A comparison between the volume fractions obtained by using the contrast available from neutron and X-ray data, Tables 5, with values derived from an analysis of X-ray data, Tables 4, highlights the differences in the two approaches.

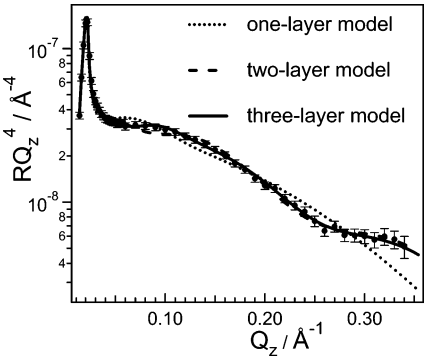

Figure 7. X-ray RQ_z^4 vs Q_z profiles obtained from β-casein spread at the air/poly(silicic) acid interface at pH 5−7, trough area ca. 200 cm^2, showing the comparison of the one-, two-, and three-layer models.

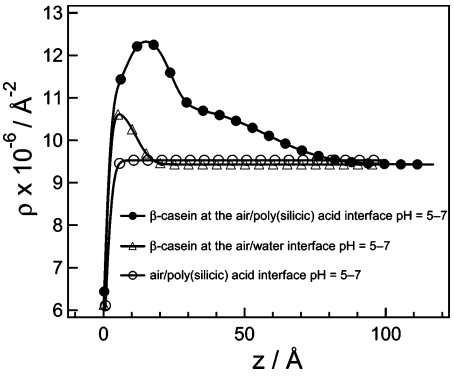

Figure 8. Scattering length density (ρ) vs depth (z) profiles from an uncompressed film of (a) β-casein spread at the air/poly(silicic) acid (closed circle) and air/water interface (open triangle), pH 5−7. The profile obtained from the air/poly(silicic) interface, pH 5−7, without spread protein (open circle) is shown. The line through each profile represents the modeled data.

One source of the discrepancy is the use of a protein density derived from an approximation of the total volume of the protein from amino acid residues, Table 1. The use of pycnometery[48] and the magnetic driver balance[49] have been shown to be precise but may not account for a layer of structured water around the surface of the molecule. Theoretical calculations have employed Voronoi polyhedra to atomic coordinates generated from single-crystal X-ray diffraction experiments.[50−53] The estimated values for protein density by these methods fall between 1.22 ± 0.02 g cm^{-1} [52] and 1.43 ± 0.03 g cm^{-1}.[53]

5. Conclusions

The interaction between β-casein spread at the air/water and a air/poly(silicic) acid subphase has been studied. Reflectometry, using neutrons and X-rays, was used in concert with a surface balance to demonstrate the pH-dependent interaction between the protein spread on a subphase containing colloidal silica. At pH 2−3 a spread protein displayed qualitatively similar monolayer behavior with no significant interaction with the siliceous subphase. Upon compression, models comprised of a single layer of constant density were no longer adequate to describe the reflectivity data, so two−three layer models were required.

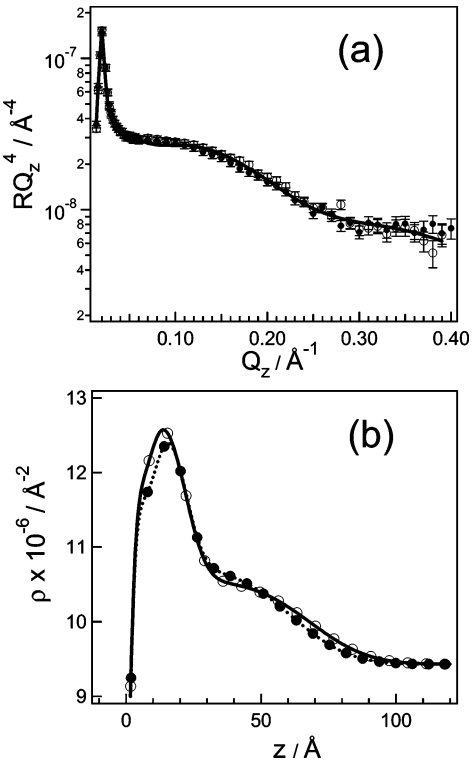

Figure 9. Comparison between ≤100% and 90% β-casein. (a) X-ray RQ_z^4 vs Q_z profiles of β-casein spread at the air/poly(silicic) acid interface, pH 5−7: β-casein ≤100% purity (closed circle) and β-casein 90% purity (open circle). (b) ρ vs depth (z) profiles of β-casein ≤100% purity (closed circle) and β-casein 90% purity (open circle).

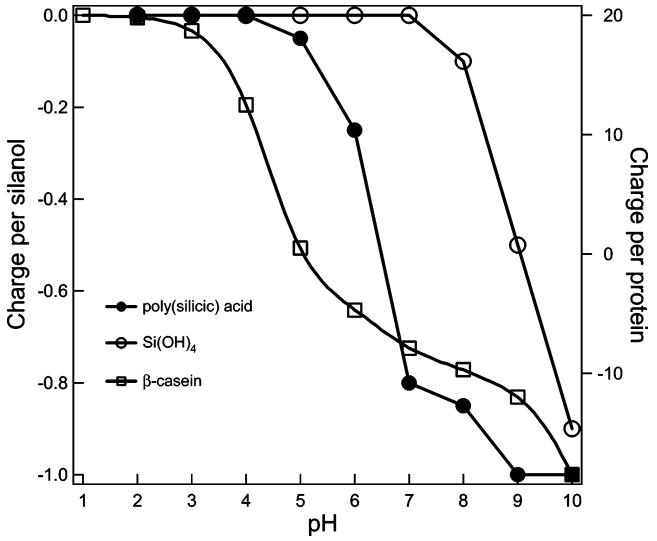

Figure 10. Plots of net on β-casein as a function of pH. Data for the charge per silanol group and poly(silicic) acids are from ref 6.

A film spread on a subphase at pH 5−7 showed strong effects on the film structure. At this pH the interface comprised three regions, a protein upper layer on top of a layer of silicated material followed by a diffuse layer that extended into the subphase. On poly(silicic) acid pH 2−3 a β-casein film when partly compressed incorporated some siliceous material, though not enough to generate a pronounced layer as shown on the poly(silicic) acid subphase at pH 5−7. On scattering length density grounds compression of the β-casein film spread on poly(silicic) acid at pH 5−7 appeared to force the dense second layer to the interface.

Acknowledgment. Dr. Tony Treloar and Mr. Jeff Herse at the Innovative Food Technologies Queensland, of the Department of Primary Industries, are acknowledged for providing a sample of purified β-casein. We thank Dr. Stephen Holt at the Rutherford Appleton Laboratory, UK, for experimental assistance. Travel to the RAL was funded through the Access to Major Facilities Program administered by ANSTO (Australian Nuclear Science and Technology Organization). Detailed criticisms by a referee are gratefully acknowledged.

References and Notes

(1) Clarke, S. G.; Holt, P. F.; Went, C. W. *Faraday Soc. Trans.* **1957**, *53*, 1500.
(2) In *National Research Council, Biomolecular self-assembling materials, Scientific and Technical Frontiers*; National Academy Press: Washington, DC, 1996.
(3) Coradin, T.; Durupthy, O.; Livage, J. *Langmuir* **2002**, *18*, 2331.
(4) Mizutani, T.; Nagase, H.; Fujiwara, N.; Ogoshi, H. *Bull. Chem. Soc. Jpn* **1998**, *71*, 2017.
(5) Mizutani, T.; Nagase, H.; Ogoshi, H. *Chem. Lett.* **1998**, 133.
(6) Coradin, T.; Coupé, A.; Livage, J. *Colloids Surf., B* **2003**, *29*, 189.
(7) Casas, M.; Minones, J.; Iribarnegaray, E. *Colloids Surf.* **1991**, *59*, 345.
(8) Casas, M.; Minones, J. *Colloid Polym. Sci.* **1992**, *270*, 478.
(9) Casas, M.; Minones, J. *Colloid Polym. Sci.* **1992**, *270*, 485.
(10) Poulsen, N.; Kröger, N. *J. Biol. Chem.* **2004**, *279*, 42993.
(11) Sumper, M.; Kroger, N. *J. Mater. Chem.* **2004**, *14*, 2059.
(12) Perry, C. C.; Keeling-Tucker, T. *J. Biol. Inorg. Chem.* **2000**, *5*, 537.
(13) Kröger, N.; Deutzmann, R.; Bergsdorf, C.; Sumper, M. *Proc. Natl. Acad. Sci. U.S.A.* **2000**, *97*, 14133.
(14) Kröger, N.; Deutzmann, R.; Sumper, M. *Science* **1999**, *286*, 1129.
(15) Shimizu, K.; Cha, J.; Stucky, G. D.; Morse, D. E. *Proc. Natl. Acad. Sci. U.S.A.* **1998**, *95*, 6234.
(16) Perry, C. C.; Keeling-Tucker, T. *Colloid Polym Sci.* **2003**, *281*, 652.
(17) Alexander, G. B. *J. Am. Chem. Soc.* **1953**, *75*, 2887.
(18) Alexander, G. B. *J. Am. Chem. Soc.* **1954**, *76*, 2094.
(19) Engelhardt, G.; Altenburg, W.; Hoebbel, D.; Wieker, W. *Z. Anorg. Allg. Chem.* **1977**, *428*, 43.
(20) Greenberg, S. A.; Chang, T. N.; Jarnutowski, R. *J. Polym. Sci.* **1962**, *58*, 147.
(21) Iler, R. K. *The Chemistry of Silica*; John Wiley & Sons: New York, 1979.
(22) Rochow, E. G. Silicon. In *Comprehensive Inorganic Chemistry*; Bailar, J. C., Emeléus, H. J., Nyholm, R., Trotman-Dickenson, A. F., Eds.; Pergamon Press: Oxford, UK, 1973.
(23) Habsuda, J.; Simon, G. P.; Cheng, Y. B.; Hewitt, D. G.; Diggins, D. R.; Toh, H.; Cser, F. *Polymer* **2002**, *43*, 4627.
(24) Carles, C.; Huet, J. C.; Ribadeau-dumas, B. *FEBS Lett.* **1988**, *229*, 265.
(25) Jenness, R. In *Milk Proteins Chemistry and Molecular Biology*; McKenzie, H. A., Ed.; Academic Press: New York, 1970; Vol. 1.
(26) Kumosinski, T. F.; Brown, E. M.; Farrell, H. M. *J. Dairy Sci.* **1993**, *76*, 931.
(27) Douillard, R.; Daoud, M.; Aguié-Béghin, V. *Curr. Opin. Colloid Interface Sci.* **2003**, *8*, 380.
(28) Cosgrove, T.; Mears, S. J.; Griffiths, P. C. *Colloids Surf., A* **1994**, *86*, 193.
(29) Atkinson, P. J.; Dickinson, E.; Horne, D. S.; Leermakers, F. A. M.; Richardson, R. M. *Ber. Bunsen-Ges. Phys. Chem.* **1996**, *100*, 994.
(30) Dickinson, E.; Euston, S. R. *Adv. Colloid Interface Sci.* **1992**, *42*, 89.
(31) Anderson, R. E.; Pande, V. S.; Radke, C. J. *J. Chem. Phys.* **2000**, *112*, 9167.
(32) Davies, D. T.; Law, A. J. R. *J. Dairy Res.* **1977**, *44*, 213.
(33) Leaver, J.; Law, A. J. R. *J. Dairy Res.* **1992**, *59*, 557.
(34) Holt, P. F.; Bowcott, J. E. L. *Biochem. J.* **1954**, *57*, 471.
(35) Brown, A. S.; Holt, S. A.; Saville, P. M.; White, J. W. *Aust. J. Phys.* **1997**, *50*, 391.
(36) Penfold, J. In *Neutron, X-ray and Light Scattering*; Lindner, P., Zemb, T., Eds.; North-Holland: Amsterdam, The Netherlands, 1991; p 223.
(37) Brown, A. S.; Holt, S. A.; Reynolds, P. A.; Penfold, J.; White, J. W. *Langmuir* **1998**, *14*, 5532.
(38) Holt, S. A.; McGillivray, D. J.; Poon, S.; White, J. W. *J. Phys. Chem. B* **2000**, *104*, 7431.
(39) Atkinson, P. J.; Dickinson, E.; Horne, D. S.; Richardson, R. M. *J. Chem. Soc., Faraday Trans.* **1995**, *91*, 2847.
(40) Jacrot, B. *Rep. Prog. Phys.* **1976**, *39*, 911.

(41) Harzallah, B.; Aguié Béghin, V.; Douillard, R.; Bosio, L. *Int. J. Biol. Macromol.* **1998**, *23*, 73.
(42) Coradin, T.; Livage, J. *Colloids Surf., B* **2001**, *21*, 329.
(43) Edler, K. J.; Brennan, T.; Roser, S. J.; Mann, S.; Richardson, R. M. *Microporous Mesoporous Mater.* **2003**, *62*, 165.
(44) Penfold, J.; Taylor, D. J. F.; Thomas, R. K.; Tucker, I.; Thompson, L. J. *Langmuir* **2003**, *19*, 7740.
(45) Taylor, D. J. F.; Thomas, R. K.; Li, P. X. *Langmuir* **2003**, *19*, 3712.
(46) Taylor, D. J. F.; Thomas, R. K.; Hines, J. D.; Humphreys, K.; Penfold, J. *Langmuir* **2002**, *18*, 9783.
(47) Taylor, D. J. F.; Thomas, R. K. *Langmuir* **2002**, *18*, 4748.
(48) McMeekin, T. L.; Groves, M. L.; Hipp, N. J. *J. Am. Chem. Soc.* **1949**, *71*, 3298.
(49) Zamyatnin, A. A. *Prog. Biophys. Mol. Biol.* **1972**, *24*, 107.
(50) Chothia, C. *Nature* **1975**, *254*, 304.
(51) Harpaz, Y.; Gerstein, M.; Chothia, C. *Structure* **1994**, *2*, 641.
(52) Andersson, K. M.; Hovmöller, S. *Z. Kristallogr.* **1998**, *213*, 369.
(53) Quillin, M. L.; Matthews, B. W. *Acta Crystallogr. D* **2000**, *56*, 791.
(54) Zamyatnin, A. A. *Annu. Rev. Biophys. Bioeng.* **1984**, *13*, 145.
(55) Sears, V. F. *Neutron News* **1992**, *3*, 26.